

tances from the origin, we may select any one location or, for symmetry, divide each spectral value by the number of equidistant images and place the resultant at each image location. After the desired manipulations, the wavenumber data may be retranslated into the array of Fig. 2 for fast inverse Fourier transformation to the lattice of Fig. 1.

ACKNOWLEDGMENT

The author wishes to thank H. Shefelbine of Sandia Corporation for his discussions on this subject.

DANIEL P. PETERSEN
Dept. of Elec. Engrg.
and Computer Sci.
University of New Mexico
Albuquerque, N. Mex. 87106

REFERENCES

- [1] J. W. Cooley and J. W. Tukey, "An algorithm for the machine calculation of complex Fourier series," *Math. Comput.*, vol. 19, pp. 297-301, 1965.
- [2] R. Bellman, *Introduction to Matrix Analysis*. New York: McGraw-Hill, 1960, p. 27.
- [3] Special Issue on Fast Fourier Transform and Its Application to Digital Filtering and Spectral Analysis, *IEEE Trans. Audio and Electroacoustics*, vol. AU-15, June 1967.
- [4] H. Miyakawa, "Sampling theorem of stationary stochastic variables in multidimensional space," *J. Inst. Elec. Commun. Engrs. Japan*, vol. 42, pp. 421-427, 1959.
- [5] D. P. Petersen and D. Middleton, "Sampling and reconstruction of wave-number-limited functions in N -dimensional Euclidean spaces," *Inform. and Control*, vol. 5, pp. 279-323, 1962.
- [6] I. N. Sneddon, *Fourier Transforms*. New York: McGraw-Hill, 1951, pp. 43-45.
- [7] D. P. Petersen and D. Middleton, "Reconstruction of multi-dimensional stochastic fields from discrete measurements of amplitude and gradient," *Inform. and Control*, vol. 7, pp. 445-476, 1964.
- [8] —, "On representative observations," *Tellus*, vol. 15, pp. 387-405, 1963.
- [9] D. P. Petersen, "On the concept and implementation of sequential analysis for linear random fields," *Tellus*, vol. 20, pp. 673-686, 1968.
- [10] G. Chrystal, *Algebra*. New York: Chelsea, 1952, p. 252.

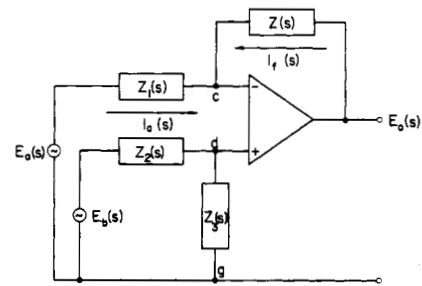


Fig. 1. Differential amplifier.

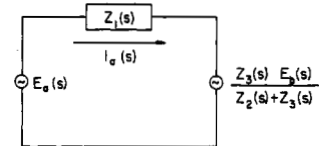


Fig. 2. Approximate equivalent circuit.

$$E_a \{ 1 + AZ / [Z + (1 + A)Z_1] \} - E_b \{ AZ_3(Z + Z_1) / [(Z_2 + Z_3)(Z + Z_1 + AZ_1)] \} = I_a(Z + Z_1). \quad (8)$$

If the two voltage sources can be linearly related by

$$E_b = KE_a \quad (9)$$

where K is assumed to be a function of the complex frequency s , then the input impedance is given by

$$Z_a = E_a / I_a = (Z_2 + Z_3)(Z + Z_1 + AZ_1) / [(1 + A)(Z_2 + Z_3) - AKZ_3]. \quad (10)$$

As $A \rightarrow \infty$, (10) becomes

$$Z_a(s) = Z_1(s) [Z_2(s) + Z_3(s)] / [Z_2(s) + Z_3(s)(1 - K(s))]. \quad (11)$$

Equation (11) indicates how the input impedance viewed by the voltage source $E_a(s)$ varies with the relationship between the two voltage sources $[K(s)]$.

A simpler derivation, which provides a better physical description of the process, can be realized if one notes that the voltage at node d can be approximately represented by an ideal voltage source

$$E_d = [Z_3 / (Z_2 + Z_3)] E_b. \quad (12)$$

Since the open-loop gain of the differential amplifier is very high,

$$E_c - E_d \approx 0. \quad (13)$$

The resulting equivalent circuit is shown in Fig. 2, and (11) follows immediately from this.

It is normally assumed that the input impedance viewed by the voltage source $E_a(s)$ is simply given as $Z_1(s)$. However, it has been shown by (11) that this is only the limiting condition when $E_b(s) = 0$ and the true impedance is a function of the relationship between the two input voltage sources. In fact, the input impedance can approach infinity if the denominator of (11) becomes zero as shown in the example which follows.

Consider the true differential or subtracting amplifier shown in Fig. 3, where the input is assumed to be two sinusoidal voltage sources of the same frequency in which the relative magnitudes and phase shift can vary. E_a is chosen as the reference so

$$K(s) = K \angle \theta_b \quad (14)$$

and

$$Z_a(s) = Z_a \angle \theta_z. \quad (15)$$

Differential Amplifier Input Impedance

Abstract—The analysis of a simple differential amplifier excited by two separate voltage sources reveals that the input impedance which loads the voltage source at the inverting input is not a constant but rather is a function of the characteristics of each voltage source. An expression is derived for the input impedance and the result is illustrated in a simple example.

Consider the differential amplifier shown in Fig. 1 where $F(s)$ is the Laplace transform of $f(t)$. The conventional model for the operational amplifier has a finite open-loop gain A , a very high impedance between nodes c and g (ground), and a very low output impedance. This model will be used to derive the input impedance viewed by the voltage source $E_a(s)$ in Fig. 1.

The basic equations are

$$E_c(s) = E_b(s) - E_d(s) \quad (1)$$

$$E_o(s) = -AE_c(s) \quad (2)$$

$$E_a(s) = I_a(s)Z_1(s) - I_f(s)Z(s) + E_o(s) \quad (3)$$

$$I_a(s) = [E_a(s) - E_c(s)] / Z_1(s) \quad (4)$$

$$I_f(s) = [E_o(s) - E_c(s)] / Z(s). \quad (5)$$

Assuming that the input impedances at the inverting ($-$) and non-inverting ($+$) input with respect to ground are high, then

$$I_a(s) \approx -I_f(s) \quad (6)$$

$$E_c(s) \approx E_b(s) + [Z_3(s) / (Z_2(s) + Z_3(s))] E_b(s). \quad (7)$$

Since all the variables are a function of the complex frequency s , it will be omitted to simplify the equations to follow.

Substituting (4), (5), and (7) into (6), solving for E_b , and substituting this into (3) gives

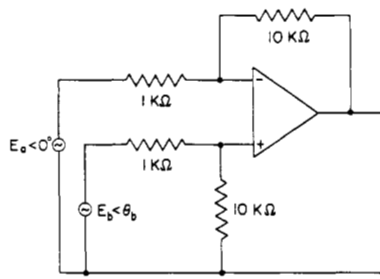


Fig. 3. Example.

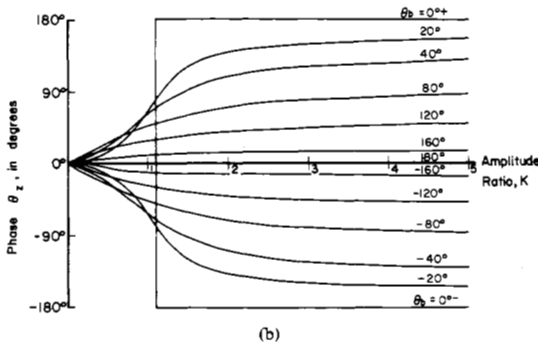
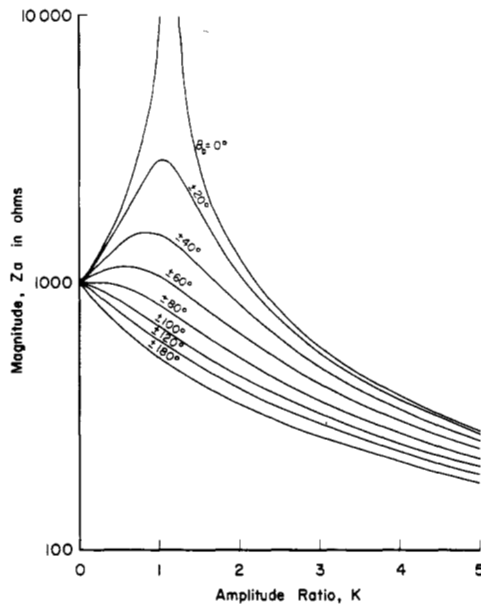


Fig. 4 (a). Impedance magnitude variations. (b). Impedance phase variations.

The variations of the magnitude Z_a and the phase θ_z with different amplitude ratios K for a constant phase shift θ_b are shown in Fig. 4.

An infinite input impedance does occur at $K = 1.1$ and $\theta_b = 0^\circ$. Also a phase reversal occurs at $K = 1.1$ for $\theta_b = 0^\circ$. Thus in designing the voltage source E_a , not only must one realize that the input impedance varies over a wide range, but also that the voltage source must be capable of current flow in both directions for correct operation of the gain characteristic. This could impose restrictions for the dc case.

To summarize, the input impedance which loads the voltage source at the inverting input of a differential amplifier excited by two voltage sources is not a constant but is a function of the characteristics of each voltage source. The expression for this variation is given in (11) and a simple interpretation is also provided. The example illustrates the effect that variations in the two voltage sources can have on the input impedance. This helps to show why the designer must consider these variations before designing such a circuit into a system.

ACKNOWLEDGMENT

The author would like to thank J. Gruber whose work provided the inspiration for this investigation, and Dr. R. B. Streets, Jr., for his comments and suggestions.

L. PAUL DENNIS
Dept. of Elec. Engrg.
University of Calgary
Calgary 44, Alberta, Canada

Zero Temperature Coefficient of Resonant Frequency in LiTaO₃ Length Expander Bars

Abstract—Zero temperature coefficient of resonant frequency has been found in LiTaO₃ length expander bars with orientations zyw (+30 deg), zyw (+35 deg), and zyw (+45 deg). These bars have large coupling constants k_{32} (more than 20 percent). The zyw (+30 deg) bar is the most promising for wide-band bandpass filter applications because it shows the smallest change in the coupling constants at ordinary temperatures.

Among the oxygen-octahedral ferroelectrics discovered in recent years, lithium tantalate is one of the most promising for applications requiring elastic and piezoelectric properties. The low temperature coefficient of frequency in a LiTaO₃ X-cut resonator was discovered by Warner *et al.* [1], and several approaches to attain the zero temperature coefficient at room temperatures have been proposed [2], [3]. Temperature characteristics of the elastic and piezoelectric properties of LiTaO₃ were studied by Smith *et al.* [4] in the temperature range from about 10° to 110°C, and also by Yamada *et al.* [5] from room temperatures up to the Curie point mainly with bar-shaped specimens. The result obtained, such as the behavior of s_{11}^E near room temperatures [5, Fig. 5(b)], immediately suggests the existence of the zero temperature coefficient of resonant frequency in the zyw (+ θ) bar with θ between 25 and 50 deg. This useful property has been confirmed by the experiments described here.

Five specimens were cut from a poled single crystal of LiTaO₃ with θ values of 25, 30, 35, 45, and 50 deg. The orientation angle θ was defined as illustrated in Fig. 1. The accuracies of the angles were checked by X-ray to be within ± 1 deg. The y' axis was taken along the length of the bars, and Ni electrodes were evaporated on the two z' faces. The dimensions of the bars were about 13.7 by 2.5 by 1.0 mm. Temperature-frequency characteristics of the five specimens are shown in Fig. 2. Zero temperature coefficients in the range 20° to 35°C are found for the zyw (+30 deg), zyw (+35 deg), and zyw (+45 deg) bars.

A resonant frequency of the length expander bar is expressed as

$$\frac{1}{(4l^2 \rho f_r)} = s_{11}^E \cos^4 \theta + s_{33}^E \sin^4 \theta + (s_{44}^E + 2s_{13}^E) \cos^2 \theta \sin^2 \theta - 2s_{14}^E \cos^3 \theta \sin \theta \tag{1}$$

where s_{ij}^E is the elastic constant at a condition of constant electric field, l the length of the bar, and ρ the density. The length of the bar is expressed as

$$l = l_0 [1 + (\alpha_2 \cos^2 \theta + \alpha_3 \sin^2 \theta) \Delta T] \tag{2}$$

where l_0 is the length of the bar at 20°C, and α_i the thermal expansion coefficient of the crystal. For LiTaO₃, $\alpha_1 = \alpha_2 = 22 \times 10^{-6}/^\circ\text{C}$, and $\alpha_3 = 1.2 \times 10^{-6}/^\circ\text{C}$ [5]. Similarly, the density is expressed as

$$\rho = \rho_0 / [(1 + \alpha_1 \Delta T) \{1 + (\alpha_2 \cos^2 \theta + \alpha_3 \sin^2 \theta) \Delta T\} \times \{1 + (\alpha_2 \sin^2 \theta + \alpha_3 \cos^2 \theta) \Delta T\}] \tag{3}$$

where ρ_0 is the density at 20°C and equal to $7.46 \times 10^3 \text{ kg/m}^3$ [5] for LiTaO₃. In (2) and (3) ΔT is the difference $(T - 20)^\circ\text{C}$. The elastic constants s_{11}^E , s_{33}^E , $(s_{44}^E + 2s_{13}^E)$, and s_{14}^E were calculated from the measured resonant frequencies of the five specimens by means of the least-squares method.